JOURNAL OF COMPUTATIONAL PHYSICS 31, 153–172 (1979)

The Laminar Boundary Layer on a Circular Cylinder Started Impulsively from Rest*

TUNCER CEBECI

Mechanical Engineering Department,
California State University at Long Beach, California 90840

Received January 20, 1978; revised May 12, 1978

A numerical method is presented for calculating the unsteady laminar flow over a circular cylinder started impulsively from rest. The governing boundary-layer equations are solved by using Keller's two-point finite-difference method. In regions where the streamwise velocity develops backflow, the solution scheme is modified by a procedure which accounts for the downstream influence. With this modification calculations were carried further in time and in space than any of the previous solutions. In particular, the calculated local skin-friction coefficients and displacement-thickness values agree with those of Belcher *et al.* Proudman and Johnson, Collins and Dennis, Bar-Lev and Yang, but do not agree with those of Telionis and Tsahalis.

INTRODUCTION

A major current problem in boundary-layer theory is to include regions of reverse crossflow or of backflow in the boundary layer. In two dimensions, the problem is associated with separation and leads to three difficulties: (a) the possible appearance of a singularity at the point of zero skin friction; (b) numerical instabilities resulting from integration opposed to the flow direction; (c) rapid thickening of the boundary layer beyond separation. In three dimensions reverse crossflow is common in flows over bodies of revolution, wings, ship hulls, etc., even though the flow remains attached in the generally accepted terminology.

There are a number of numerical procedures available for solving the boundary-layer equations in these situations (e.g., our aim in this paper is to develop an alternative and hopefully more efficient and accurate method). Of course, separation lines may occur and genuine backflow set in beyond them (i.e., both streamwise and cross-stream profiles exhibit reverse flow) but we shall not consider such regions. Rather, we confine our attention to the crucial questions remaining in the region upstream of separation where there is reverse crossflow but there is no doubt about the validity of the boundary-layer equations.

The problem we have chosen to test the new procedure is the unsteady two-dimensional laminar flow over a circular cylinder started impulsively from rest.

* This work was supported by the Office of Naval Research under contract N00014-77-C-0156.

0021-9991/79/050153-20$02.00/0

(This flow problem is roughly analogous to a three-dimensional reverse crossflow problem if we associate time with the direction of a mainstream with unit velocity component. The unsteady boundary layer is then the cross velocity.) This flow has received considerable attention in the past, the present state of knowledge being given in the recent paper by Bar–Lev and Yang [1]. Since the velocity profile contains regions of backflow, for $t > 0.320$, in which the thickness of the boundary layer rapidly increases, the computational problem posed may be viewed as one step more complex than the problem of two-dimensional steady flows, and as a good test case to study the computational procedures which may eventually be used for steady three-dimensional flows in which the crossflow contains regions of backflow. A crucial feature of the method used here for dealing with backflow is the introduction of the zigzag procedure employed by Krause, Hirschel, and Bothmann [12] into the Box method (Keller [11]) for solving parabolic equations. We note that earlier Phillips and Ackerberg [13] has used a method for computing boundary layers with backflow which may be regarded as a different combination of these two procedures.

In addition, the results are of interest in a wider and more fundamental context. First, let us consider briefly the phenomenon of dynamic stall of which a penetrating study has been recently published by Carr, McAlister, and McCroskey [5]. It arises during the slow oscillation cycle of a pitching airfoil through angles of incidence which would provoke stall under steady conditions. Although it is extremely complicated, depending in a subtle way on a large number of parameters, one characteristic feature is the formation of a large vortex near the surface just before the occurrence of stall. This vortex is clearly associated with flow reversals in the unsteady boundary layer and a reliable method of describing it is a vital feature of any predictive theory of dynamic stall. The present studies may be regarded as a step towards such a goal.

Second, there is a controversy in the literature concerning the occurrence of singularities in unsteady boundary layers (Sears and Telionis [17], Riley [15], Bar–Lev and Yang [1], Williams [21]). Sears and Telionis have advanced the view that an evolving boundary layer can develop a singularity at a specific time t_0, i.e., for $t < t_0$ the boundary layer may be computed over the entire spatial range of interest but for $t > t_0$ the integration from the forward attachment point is terminated by the appearance of a singularity at some station downstream. The best supporting evidence for this suggestion is provided by Bodonyi and Stewartson [4] who studied the growing boundary layer between two rotating discs, one of which has its angular velocity impulsively reversed in sign. However, the breakdown in the solution is quite different from that envisaged by Sears and Telionis since the velocity components and the boundary-layer thickness all become infinite together. Sears and Telionis illustrate their ideas with examples the most definite of which is the one studied in this paper. A numerical investigation has also been carried out by Telionis and Tsahalis [18] who conclude that the solution develops a singularity at $t_0 \simeq 0.65$ at a station $\theta \simeq 140°$ from the stagnation point. This result disagrees with the previous studies of Robins, reported in Belcher, Burggraf, Cooke, Robins, and Stewartson [2] and of Collins and Dennis [8, 9]. These authors found no singularity in the solution for $t < 1$. In our calculations, special care was taken to make sure no irregularity was missed due to

coarse numerical procedures but we failed to observe the singularity reported by Telionis and Tsahalis [18]. Instead we find that the solution is completely smooth for all $t < 1.4$, at which time the calculation was terminated only because the shear layer became too thick to handle efficiently by the methods of this paper. In a subsequent paper we hope to describe modifications in the computational procedure which enable us to carry out the integration to much larger values of t.

Basic Equations

Governing Equations

We consider an incompressible unsteady laminar flow over a circular cylinder started impulsively from rest. The governing boundary-layer equations and their boundary conditions for this flow are well known; see for example, Cebeci and Bradshaw [6]. They are given by

$$\frac{\partial u}{\partial x} + \frac{\partial v}{\partial y} = 0, \tag{1}$$

$$\frac{\partial u}{\partial t} + u\frac{\partial u}{\partial x} + v\frac{\partial u}{\partial y} = u_e\frac{du_e}{dx} + \nu\frac{\partial^2 u}{\partial y^2}, \tag{2}$$

$$y = 0, \qquad u = v = 0; \qquad y \to \infty, \qquad u \to u_e(x). \tag{3}$$

Starting the flow impulsively from rest leads to a singularity at $t = 0$. This can be avoided by using an appropriate similarity variable:

$$\eta = y/(\nu t)^{1/2} \tag{4}$$

and the stream function ψ for which

$$u = \frac{\partial \psi}{\partial y}, \qquad v = -\frac{\partial \psi}{\partial x}. \tag{5}$$

A dimensionless stream function $f(x, \eta, t)$ is defined by

$$\psi = (\nu t)^{1/2} u_e(x) f(x, \eta, t). \tag{6}$$

Now Eqs. (1)–(3) become (primes denote differentiation with respect to η)

$$f''' + \frac{\eta}{2}f'' + t\frac{du_e}{dx}[1 - (f')^2 + ff''] = t\left[\frac{\partial f'}{\partial t} + u_e\left(f'\frac{\partial f'}{\partial x} - f''\frac{\partial f}{\partial x}\right)\right], \tag{7}$$

$$\eta = 0, \qquad f = f' = 0; \qquad \eta = \eta_\infty, \qquad f' = 1. \tag{8}$$

These variables are employed only for some interval $0 \leqslant t \leqslant t_*$ during which the boundary layer rapidly develops. For $t \geqslant t_*$ we switch to other dimensionless variables Y and F defined by

$$Y = y/L, \qquad \psi = u_e L F(x, Y, t). \tag{9}$$

Equations (1)–(3) now become

$$F''' + \frac{du_e}{dx}[1 - (F')^2 + FF''] = \frac{\partial F'}{\partial t} + u_e\left(F'\frac{\partial F'}{\partial x} - F''\frac{\partial F}{\partial x}\right), \tag{10}$$

$$Y = 0, \qquad F = F' = 0; \qquad Y = Y_\infty, \qquad F' = 1. \tag{11}$$

Here L is a reference length, x, t, and u_e are nondimensional quantities defined by x/L, $u_\infty t/L$, and u_e/u_∞, respectively, and the primes denote differentiation with respect to Y.

Initial Conditions

The solution of the governing equations described above requires initial conditions along the (x, y) and (t, y) planes. In the former case, they can be obtained from (7), which for $t = 0$, reduces to

$$f''' + \tfrac{1}{2}\eta f'' = 0. \tag{12}$$

The solution of Eq. (12) subject to (8) is given by

$$\begin{aligned} f &= \eta\,\mathrm{erf}\left(\frac{\eta}{2}\right) + \frac{2}{\pi^{1/2}}\left[\exp\left(-\frac{\eta^2}{4}\right) - 1\right], \\ f' &= \mathrm{erf}\left(\frac{\eta}{2}\right), \qquad f'' = \frac{1}{\pi^{1/2}}\exp\left(-\frac{\eta^2}{4}\right). \end{aligned} \tag{13}$$

The initial conditions along the (t, y) plane at the forward and rear stagnation points can be obtained from (7) and (10). The external flow is given by

$$u_e = (1/\pi)\sin \pi x. \tag{14}$$

Then for $t > 0$ at $x = 0$ and $x = 1$, Eqs. (7) and (10) become

$$f''' + \frac{\eta}{2}f'' + t\lambda[1 - (f')^2 + ff''] = t\frac{\partial f'}{\partial t}, \tag{15}$$

$$F''' + \lambda[1 - (F')^2 + FF''] = \frac{\partial F'}{\partial t}, \tag{16}$$

where $\lambda = 1$ for $x = 0$ and $\lambda = -1$ for $x = 1$.

Numerical Method

We use Keller's two-point finite-difference method (called the Box method) to solve the system of equations described in the previous section. The application of this method to steady and unsteady two-dimensional flows and to steady three-dimensional flows with backflow are described in several references, see for example, Cebeci and

Bradshaw [6]. Here we describe its application to unsteady two-dimensional flows with backflow following a brief description of the method for flows with no backflow (standard Box method). For simplicity we only discuss the numerical method for the solution of (7) and (8) for $t > 0$ and $0 < x < 1$.

Standard Box Method

To solve (7) and (8) by the standard Box method, we first write (7) in terms of a system of first-order equations by introducing new dependent variables $u(x, \eta, t)$, $v(x, \eta, t)$, that is,

$$f' = u, \tag{17a}$$

$$u' = v, \tag{17b}$$

$$v' + \frac{\eta}{2} v + \lambda(1 - u^2 + fv) = t\left[\frac{\partial u}{\partial t} + u_e\left(u\frac{\partial u}{\partial x} - v\frac{\partial f}{\partial x}\right)\right], \tag{17c}$$

where $\lambda \equiv t\, du_e/dx$. Note that these variables u and v are new definitions and are not related to those defined previously in Eqs. (1)–(4). We next consider the net cube shown in Fig. 1 and denote the net points by

$$\begin{aligned} x_0 &= 0, \quad & x_i &= x_{i-1} + r_i, \\ t_0 &= 0, \quad & t_n &= t_{n-1} + k_n, \\ \eta_0 &= 0, \quad & \eta_j &= \eta_{j-1} + h_j \end{aligned} \tag{18}$$

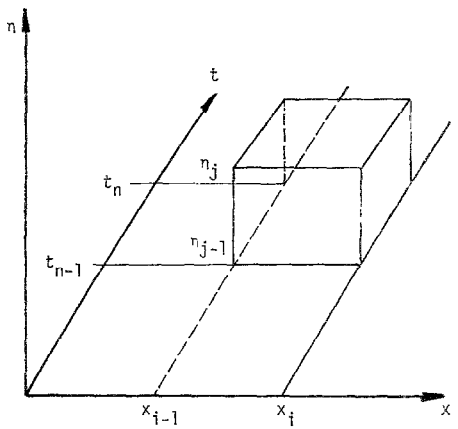

FIG. 1. Net cube for the standard Box method.

for values of i, n, and j starting from 1, 2,..., to I, N, and J, respectively. For the net points given by (18), we approximate the quantities (f, u, v) at points (x_i, t_n, η_j) by the net functions denoted by $(f_j^{i,n}, u_j^{i,n}, v_j^{i,n})$. Equations (17a) and (17b) are approx-

imated using centered difference quotients and averaged about the midpoint $(x_i, t_n, \eta_{j-1/2})$, that is,

$$h_j^{-1}(f_j^{i,n} - f_{j-1}^{i,n}) = u_{j-1/2}^{i,n}, \tag{19a}$$

$$h_j^{-1}(u_j^{i,n} - u_{j-1}^{i,n}) = v_{j-1/2}^{i,n}, \tag{19b}$$

where, for example,

$$u_{j-1/2}^{i,n} \equiv \tfrac{1}{2}(u_j^{i,n} + u_{j-1}^{i,n}).$$

The difference equations which are to approximate (17c) are written about the midpoint $(x_{i-1/2}, t_{n-1/2}, \eta_{j-1/2})$ of the cube whose mesh widths are r_i, k_n, and h_j.

$$\begin{aligned} h_j^{-1}(\bar{v}_j - \bar{v}_{j-1}) + \tfrac{1}{2}\eta_{j-1/2}\bar{v}_{j-1/2} + \bar{\lambda}[1 - (\overline{u^2})_{j-1/2} + (\overline{fv})_{j-1/2}] \\ = \beta_n(\bar{u}_k - \bar{u}_{k-1}) + \alpha_i[\bar{u}_{j-1/2}(\bar{u}_i - \bar{u}_{i-1}) - \bar{v}_{j-1/2}(\bar{f}_i - \bar{f}_{i-1})], \end{aligned} \tag{19c}$$

where, for example,

$$\begin{aligned} \bar{v}_j &= \tfrac{1}{4}(v_j^{i,n} + v_j^{i-1,n} + v_j^{i-1,n-1} + v_j^{i,n-1}) = \tfrac{1}{4}(v_j^{i,n} + v_j^{234}), \\ \bar{u}_i &= \tfrac{1}{2}(u_{j-1/2}^{i,n} + u_{j-1/2}^{i,n-1}), \qquad \bar{u}_n = \tfrac{1}{2}(u_{j-1/2}^{i,n} + u_{j-1/2}^{i-1.n}), \end{aligned} \tag{20}$$

and

$$\beta_n = \frac{t^{n-1/2}}{k_n}, \qquad \alpha_i = u_e^{i-1/2}\frac{t^{n-1/2}}{r_i}, \qquad \bar{\lambda} = \lambda_{i-1/2}^{n-1/2}. \tag{21}$$

Here by v_j^{234} we mean $v_j^{234} = v_j^{i-1,n} + v_j^{i-1,n-1} + v_j^{i,n-1}$, the sum of the values of v_j at three of the four corners of the face of the box.

Introducing (20) and similar definitions for other terms into (19c), after considerable algebra, we get

$$\begin{aligned} h_j^{-1}(v_j - v_{j-1}) + \tfrac{1}{2}\eta_{j-1/2}v_{j-1/2} + \bar{\lambda}[(fv)_{j-1/2} - (u^2)_{j-1/2}] - 2\beta_n u_{j-1/2} \\ - \tfrac{1}{2}\alpha_i[(u_{j-1/2})^2 + (m_1 + m_6)\,u_{j-1/2} - v_{j-1/2}f_{j-1/2} - m_3 f_{j-1/2} - m_4 v_{j-1/2}] = m_7. \end{aligned} \tag{22}$$

Here for convenience we have dropped the superscripts i and n and have defined

$$\begin{aligned} m_1 &= u_{j-1/2}^{234}, \qquad m_2 = u_{j-1/2}^{(2)} - 2\bar{u}_{n-1}, \qquad m_3 = v_{j-1/2}^{234}, \qquad m_4 = f_{j-1/2}^{(4)} - 2\bar{f}_{i-1}, \\ m_5 &= (u^2)_{j-1/2}^{234}, \qquad m_6 = u_{j-1/2}^{(4)} - 2\bar{u}_{i-1}, \\ m_7 &= -h_j^{-1}(v_j^{234} - v_{j-1}^{234}) - \tfrac{1}{2}\eta_{j-1/2}m_3 - \bar{\lambda}[4 - m_5 + (fv)_{j-1/2}^{234}] \\ &\quad + 2\beta_n m_2 + \tfrac{1}{2}\alpha_i(m_1 m_6 - m_3 m_4). \end{aligned} \tag{23}$$

The boundary conditions in (8) become

$$f_0 = 0, \qquad u_0 = 0, \qquad u_J = 1. \tag{24}$$

The algebraic system given by (19a), (19b), (22), and (24) is nonlinear. To linearize it we use Newton's method and introduce the iterates $[f_j^{(\nu)}, u_j^{(\nu)}, v_j^{(\nu)}]$, $\nu = 0, 1, 2,...$, with initial values, say,

$$f_0^{(0)} = 0, \qquad u_0^{(0)} = 0, \qquad v_0^{(0)} = v_0^{i-1,n},$$
$$f_j^{(0)} = f_j^{i-1,n}, \qquad u_j^{(0)} = u_j^{i-1,n}, \qquad v_j^{(0)} = v_j^{i-1,n}, \qquad 1 \leqslant j \leqslant J-1, \tag{25}$$
$$f_J^{(0)} = f_J^{i-1,n}, \qquad u_J^{(0)} = 1, \qquad v_J^{(0)} = v_J^{i-1,n}.$$

For the higher-order iterates we set

$$f_j^{(\nu+1)} = f_j^{(\nu)} + \delta f_j^{(\nu)}, \qquad u_j^{(\nu+1)} = u_j^{(\nu)} + \delta u_j^{(\nu)}, \qquad v_j^{(\nu+1)} = v_j^{(\nu)} + \delta v_j^{(\nu)}. \tag{26}$$

Then we insert the right-hand sides of these expressions in place of f_j, u_j, and v_j in Eqs. (19a), (19b), and (22) and drop the terms that are quadratic in $(\delta f_j^{(\nu)}, \delta u_j^{(\nu)}, \delta v_j^{(\nu)})$. This procedure yields the following linear system written in a form identical to that in Cebeci and Bradshaw [6]:

$$\delta f_j - \delta f_{j-1} - \tfrac{1}{2}h_j(\delta u_j + \delta u_{j-1}) = (r_1)_j, \tag{27a}$$
$$\delta u_j - \delta u_{j-1} - \tfrac{1}{2}h_j(\delta v_j + \delta v_{j-1}) = (r_3)_{j-1}, \tag{27b}$$
$$(s_1)_j\,\delta v_j + (s_2)_j\,\delta v_{j-1} + (s_3)_j\,\delta f_j + (s_4)_j\,\delta f_{j-1} + (s_5)_j\,\delta u_j + (s_6)_j\,\delta u_{j-1} = (r_2)_j. \tag{27c}$$

Here for convenience we have dropped the superscript ν in δ quantities and have defined $(r_1)_j$, $(r_2)_j$, $(r_3)_j$, and $(s_1)_j$–$(s_6)_j$ by

$$(r_1)_j = f_{j-1} - f_j + h_j u_{j-1/2}, \tag{28a}$$
$$(r_3)_{j-1} = u_{j-1} - u_j + h_j v_{j-1/2}, \tag{28b}$$
$$(r_2)_j = m_7 - [h_j^{-1}(v_j - v_{j-1}) + \tfrac{1}{2}\eta_{j-1\,2}v_{j-1/2} + \gamma\{(fv)_{j-1\cdot 2} - (u^2)_{j-1\cdot 2}\} - 2\beta_n u_{j-1\,2}$$
$$- \tfrac{1}{2}\alpha_i\{(u_{j-1/2})^2 + (m_1 + m_6)\,u_{j-1/2} - v_{j-1/2}f_{j-1\,2} - m_3 f_{j-1\cdot 2} - m_4 v_{j-1\cdot 2}\}]. \tag{28c}$$
$$(s_1)_j = 1/h_j + \tfrac{1}{4}\eta_{j-1/2} + \tfrac{1}{2}\gamma f_j + \tfrac{1}{4}\alpha_i(f_{j-1/2} + m_4), \tag{29a}$$
$$(s_2)_j = -1/h_j + \tfrac{1}{4}\eta_{j-1/2} + \tfrac{1}{2}\gamma f_{j-1} + \tfrac{1}{4}\alpha_i(f_{j-1/2} + m_4), \tag{29b}$$
$$(s_3)_j = \tfrac{1}{2}\gamma v_j + \tfrac{1}{4}\alpha_i(v_{j-1/2} + m_3), \tag{29c}$$
$$(s_4)_j = \tfrac{1}{2}\gamma v_{j-1} + \tfrac{1}{4}\alpha_i(v_{j-1/2} + m_3), \tag{29d}$$
$$(s_5)_j = -\gamma u_j - \beta_n - \tfrac{1}{4}\alpha_i(2u_{j-1\,2} + m_1 + m_6), \tag{29e}$$
$$(s_6)_j = -\gamma u_{j-1} - \beta_n - \tfrac{1}{4}\alpha_i(2u_{j-1\cdot 2} + m_1 + m_6). \tag{29f}$$

Here

$$\gamma = t^{n-1/2}\left(\frac{du_e}{dx}\right)_{i-1/2} \tag{30}$$

Similarly the boundary conditions (24) become

$$\delta f_0 = 0, \qquad \delta u_0 = 0, \qquad \delta u_J = 0. \tag{31}$$

Equations (27) and (31) form an implicit linear algebraic system of $3J + 3$ equations in as many unknowns ($f_j^{i,n}$, $u_j^{i,n}$, $v_j^{i,n}$) with i and $n \geqslant 1$. The initial conditions at $n = 0$ for all i are obtained from (13) and those at $i = 0$ are obtained from the solution of (17) and (8) for all $n > 1$. In the latter case, a similar procedure described above and in detail in Cebeci and Bradshaw [6] was used to express the differenced linearized equations in a form identical to (27) and (31) except now

$$(r_2)_j = R_{j-1/2} - [v_{j-1/2} + \tfrac{1}{2}\eta_{j-1/2}v_{j-1/2} + \tilde{\lambda}\{1 - (u^2)_{j-1/2} + (fv)_{j-1/2}\} - 2\beta_n u_{j-1/2}]^{i,n}, \tag{32a}$$

$$R_{j-1/2} = -[v_{j-1/2} + \tfrac{1}{2}\eta_{j-1/2}v_{j-1/2} + \tilde{\lambda}\{1 - (u^2)_{j-1/2} + (fv)_{j-1/2}\}]^{i,n-1} - 2\beta_n u_{j-1/2}^{i,n-1}, \tag{32b}$$

$$\tilde{\lambda} \equiv t\lambda, \tag{32c}$$

and

$$(s_1)_j = 1/h_j + \tfrac{1}{4}\eta_{j-1/2} + \tfrac{1}{2}\tilde{\lambda}f_j, \tag{33a}$$

$$(s_2)_j = -1/h_j + \tfrac{1}{4}\eta_{j-1/2} + \tfrac{1}{2}\tilde{\lambda}f_{j-1}, \tag{33b}$$

$$(s_3)_j = \tfrac{1}{2}\tilde{\lambda}v_j, \tag{33c}$$

$$(s_4)_j = \tfrac{1}{2}\tilde{\lambda}v_{j-1}, \tag{33d}$$

$$(s_5)_j = -\tilde{\lambda}u_j - \beta_n, \tag{33e}$$

$$(s_6)_j = -\tilde{\lambda}u_{j-1} - \beta_n. \tag{33f}$$

The linear systems for Eqs. (17) and (8) are obtained by using the block-elimination method discussed by Keller [11] and by Cebeci and Bradshaw [6].

Modified Box Method

The solution of the momentum equation (7) and (8) is obtained by the standard Box method for a given time $t = t_n$ by marching in the x-direction. Since the linearized form of the equations is being solved, the solutions are iterated at each x-station until a convergence criterion based on the wall-shear parameter f_w'' is satisfied, that is,

$$|(f_w'')^{\nu+1} - (f_w'')^{\nu}| = |\delta f_w''| < \delta_1. \tag{34}$$

Here δ_1 is a specified number which was set equal to 10^{-6} in the calculations.

All previous boundary-layer calculations were done for the external velocity distribution given by

$$u_e = 2u_\infty \sin x. \tag{35}$$

whereas ours used (14). The change in the definitions of u_e and x implies that our time scale differs from that used previously by a factor of 2. For consistency we shall continue to use t for our time and T for that of others with $2T = t$.

In order to perform the calculations for a flow with regions of backflow, it is obvious that some upstream influence must be allowed when the streamwise velocity changes sign. In our problem the first appearance of the flow reversal around the circular cylinder occurs at $t > 0.50$. For this reason we take $t_* = \frac{1}{4}$ so that flow reversal occurs only when we use the physical variables (9)–(11).

The solution of the system (10), (11), and (16) for the case when there is no flow reversal is very similar to the solution of the system given by (7), (8), and (15). Again we introduce new dependent variables $U(x, Y, t)$ and $V(x, Y, t)$ and, with λ now denoting du_e/dx, we write (10) as

$$F' = U, \tag{36a}$$

$$U' = V, \tag{36b}$$

$$V' + \lambda(1 - U^2 + FV) = \frac{\partial U}{\partial t} + u_e\left(U\frac{\partial U}{\partial x} - V\frac{\partial F}{\partial x}\right). \tag{36c}$$

When there is no flow reversal, the difference equations for the above system are very similar to those given by (17). As a matter of fact if we replace f, u, and v in Eqs. (19)–(31) by F, U, and V, we can use the same coefficients $(r_1)_j$–$(r_3)_j$ and $(s_1)_j$–$(s_6)_j$ provided that we now redefine γ, β_n, α_i, and h_j by

$$\gamma \equiv \left(\frac{du_e}{dx}\right)_{i-1/2}, \qquad \beta_n = \frac{1}{k_n}, \qquad \alpha_i = \frac{u^{i-1/2}}{r_i}, \qquad h_j = \Delta Y_j. \tag{37}$$

In addition we set $\eta_{j-1/2}$ in (28c), (29a), and (29b) equal to zero.

Similarly we can solve (16) and (11) by using the solution algorithm described for (15) and (8) again by making minor modifications to those coefficients given in (32) and (33). As before we set the term $\eta_{j-1/2}$ in (32a), (32b), (33a), and (33b) equal to zero. We also let β_n be given by that in (37) and set $\tilde{\lambda} = \lambda$.

When there is flow reversal across the boundary layer at some x and t, then we modify our procedure used in the standard Box method for Eq. (36c) but we still keep the previous procedure for Eqs. (36a) and (36b) and center them at $(x_i, t_n, Y_{j-1/2})$ to get

$$h_j^{-1}(F_j^{i,n} - F_{j-1}^{i,n}) = U_{j-1/2}^{i,n}, \tag{38a}$$

$$h_j^{-1}(U_j^{i,n} - U_{j-1}^{i,n}) = V_{j-1/2}^{i,n}. \tag{38b}$$

To write the difference approximations for the Box centered at $(x_{i-1/2}, t_{n-1/2}, Y_{j-1/2})$ we examine previously computed values of $U^{i,n}_{j-1/2}$. If $U^{i,n}_{j-1/2} \geqslant 0$, then we use the standard Box method described before. If $U^{i,n}_{j-1/2} < 0$, then we write (36c) for the Box centered at P (see Fig. 2) using quantities centered at P, Q, and R, where

$$P \equiv (x_i, t_{n-1/2}, Y_{j-1/2}), \quad Q \equiv (x_{i-1/2}, t_n, Y_{j-1/2}), \quad R \equiv (x_{i+1/2}, t_{n-1}, Y_{j-1/2}). \tag{39}$$

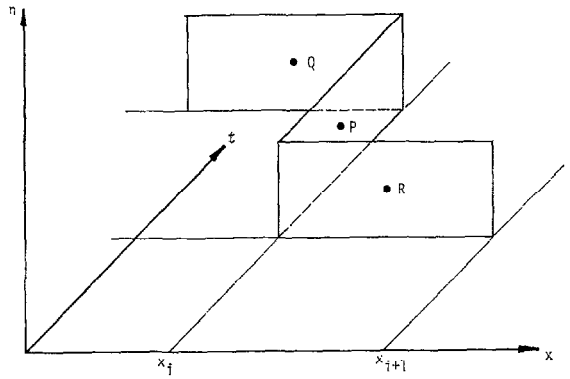

FIG. 2. Finite difference molecule for the zigzag differencing.

Equation (36c) can then be written as

$$\begin{aligned} &V'(P) + \lambda(P)[1 - U^2(P) + (FV)(P)] \\ &\quad = \frac{\partial U}{\partial t}(P) + u_e(P)\left[\theta U(Q)\frac{\partial U}{\partial x}(Q) + \phi U(R)\frac{\partial U}{\partial x}(R)\right. \\ &\quad\quad \left. - \left\{\theta V(Q)\frac{\partial F}{\partial x}(Q) + \phi V(R)\frac{\partial F}{\partial x}(R)\right\}\right]. \end{aligned} \tag{40}$$

Here

$$\theta \equiv \frac{x_{i+1} - x_i}{x_{i+1} - x_{i-1}}, \qquad \phi = \frac{x_i - x_{i-1}}{x_{i+1} - x_{i-1}}. \tag{41}$$

The difference equations which are to approximate (40) are

$$\begin{aligned} &h_j^{-1}(V_j^{i,n-1/2} - V_{j-1}^{i,n-1/2}) + \lambda^i[1 - (U^2)_{j-1/2}^{i,n-1/2} + (FV)_{j-1/2}^{i,n-1/2}] \\ &\quad = k_n^{-1}(U_{i-1/2}^{i,n} - U_{j-1/2}^{i,n-1}) \\ &\quad\quad + u_e{}^i\bar{\theta}[U_{j-1/2}^{i-1/2,n}(U_{j-1/2}^{i,n} - U_{j-1/2}^{i-1,n}) - V_{j-1/2}^{i-1/2,n}(F_{j-1/2}^{i,n} - F_{j-1/2}^{i-1,n})] + \beta_2 . \end{aligned} \tag{42}$$

Here

$$\tilde{\theta} = \frac{r_{i+1}}{r_i}\frac{1}{(x_{i+1} - x_{i-1})}, \tag{43}$$

$$\beta_2 = -\frac{u_e{}^i r_i}{(x_{i+1} - x_{i-1})^2}\left[U_{j-1/2}^{i+1/2,n-1}(U_{j-1/2}^{i,n-1} - U_{j-1/2}^{i+1,n-1}) - V_{j-1/2}^{i+1/2,n-1}(F_{j-1/2}^{i,n-1} - F_{j-1/2}^{i+1,n-1})\right], \tag{44}$$

After considerable algebra it can be shown that (42) can be written as

$$h_j^{-1}(V_j - V_{j-1}) + \lambda_i[(FV)_{j-1/2} - (U^2)_{j-1/2}] - 2k_n^{-1}U_{j-1/2}$$
$$- u_e{}^i\tilde{\theta}[(U_{j-1/2})^2 - V_{j-1/2}F_{j-1/2} + F_{j-1/2}^{i-1,n}V_{j-1/2} - V_{j-1/2}^{i-1,n}F_{j-1/2}] = 2\beta_3, \tag{45}$$

where again we have dropped the superscripts i and n in the above equation and have defined

$$\beta_3 = -\tfrac{1}{2}h_j^{-1}(V_j^{i,n-1} - V_{j-1}^{i,n-1}) - \tfrac{1}{2}\lambda_i[(FV)_{j-1/2}^{i,n-1} - (U^2)_{j-1/2}^{i,n-1}] - k_n^{-1}U_{j-1/2}^{i,n-1}$$
$$+ \beta_2 + \tfrac{1}{2}u_e{}^i\tilde{\theta}[-(U_{j-1/2})^2 + V_{j-1/2}F_{j-1/2}]. \tag{46}$$

The system (38a), (38b), (45), and the boundary conditions

$$F_0 = 0, \qquad U_0 = 0, \qquad U_J = 1 \tag{47}$$

can again be linearized by using Newton's method and be placed in a form identical to those given by (27) and (31) except now

$$(r_2)_j = 2\beta_3 - [V'_{j-1/2} + \lambda_i\{(FV)_{j-1/2} - (U^2)_{j-1/2}\} - 2\beta_n U_{j-1/2}$$
$$- u_e{}^i\tilde{\theta}\{(U_{j-1/2})^2 - V_{j-1/2}F_{j-1/2} + F_{j-1/2}^{i-1,n}V_{j-1/2} - V_{j-1/2}^{i-1,n}F_{j-1/2}\}], \tag{48}$$

$$(s_1)_j = 1/h_j + \tfrac{1}{2}\lambda_i F_j - \tfrac{1}{2}u_e{}^i\tilde{\theta}(-F_{j-1/2} + F_{j-1/2}^{i-1,n}), \tag{49a}$$

$$(s_2)_j = -1/h_j + \tfrac{1}{2}\lambda_i F_{j-1} - \tfrac{1}{2}u_e{}^i\tilde{\theta}(-F_{j-1/2} + F_{j-1/2}^{i-1,n}), \tag{49b}$$

$$(s_3)_j = \tfrac{1}{2}\lambda_i V_j + \tfrac{1}{2}u_e{}^i\tilde{\theta}(V_{j-1/2} + V_{j-1/2}^{i-1,n}), \tag{49c}$$

$$(s_4)_j = \tfrac{1}{2}\lambda_i V_{j-1} + \tfrac{1}{2}u_e{}^i\tilde{\theta}(V_{j-1/2} + V_{j-1/2}^{i-1,n}), \tag{49d}$$

$$(s_5)_j = -\lambda_i U_j - \beta_n - u_e{}^i\tilde{\theta}U_{j-1/2}, \tag{49e}$$

$$(s_6)_j = -\lambda_i U_{j-1} - \beta_n - u_e{}^i\tilde{\theta}U_{j-1/2}. \tag{49f}$$

Results and Discussion

The velocity field for a laminar flow over a circular cylinder started impulsively from rest has been computed by using both Navier–Stokes equations and by boundary-layer equations. The earliest numerical study of the boundary-layer equation was carried out by Robins (see Belcher *et al.* [2]) who found that the skin friction vanished at an interior point x_0 of (0, 1) for $T > T_s$ where T_s is a finite positive number. (They quote a value of 0.377 for T_s which appears to be a misprint; the correct value is $\simeq$0.320.) At $T = T_s$, $x_0 = 1$ (the rear stagnation point) and subsequently x_0 decreases eventually approaching the value $1.82\pi^{-1}$ given by the steady-state solution (Terrill [19]). Their results were obtained by using a Crank–Nicholson implicit method. For cases with no backflow, they used the standard form of this method. For cases with backflow they modified their scheme by computing the values of u at a new station of T from the values of u at the *two* previous stations of T, and neighboring points on the x-grid both upstream and downstream. The modified method was thus three tier instead of two tier, as their standard method. The time step was 0.025, the x-step 1/18 (=10°) and the y-step 0.1. They found it was possible to carry the solution procedure forward to $T = 1$ before the results become too unreliable. In fact, inaccuracies began to develop at $T = 1$ near the stagnation point and spread in both directions of x.

According to a similar study conducted by Telionis and Tsahalis, the time required for zero skin friction to appear at the rear stagnation point agrees with the calculations of Blasius [3]; that is, $T = 0.35$. With their numerical method, modified to account for the backflow, they determined the location of zero skin friction for later times and observed that, for $T < 1$, their predictions agreed well with those of Thoman and Szewczyk [20] based on the solution of Navier–Stokes equations. For $T > 1.0$, they were not able to obtain solutions. For $0.35 \leqslant T \leqslant 0.65$, they calculated the flow field up to $x \cong 1$ (=180°). At about $T \cong 0.65$, and in the neighborhood of $x \simeq 0.77$ (=140°) they claimed that a singularity appeared and were only able to obtain solutions for a few more x-stations beyond the one that corresponds to zero skin friction. They attributed this failure to compute more stations in the downstream flow to "a natural response of the boundary-layer model to separation as predicted by Sears and Telionis [16] and not to a mere creature of the particular numerical procedure adopted."

Recently Bar-Lev and Yang [1] solved the full Navier–Stokes equations for the same problem by the method of matched asymptotic expansions. Analytical solutions for the stream function in terms of exponential and error functions for the inner flow field and of circular functions for the outer were obtained to the third order, from which a uniformly valid composite solution was found. Their calculated quantities which included vorticity, pressure, separation point, and drag agreed well with the numerical computations of Collins and Dennis [8, 9]. As did Collins and Dennis, they observed the zero wall shear to occur at $T = 0.322$ at the rear stagnation point.

In the calculations reported here, we first used the standard Box method to calculate the flow field for $\Delta t = 0.05$ and for $\Delta x = 0.025$, corresponding to 41 x-stations

spaced 4.5° around the circular cylinder. For $t < t_*$ we set $\Delta\eta = 0.1$, $\eta_\infty = 10$, thus taking 101 η-points across the boundary layer. At first we chose $t_* = 1$ and switched to the physical variables at $t > 1$. We let the boundary-layer thickness Y_∞ grow with t with ΔY uniform and equal to 0.1. By first using the standard Box method, we attempted to quantify the range of possible calculations, with and without backflow. With this standard procedure we were able to calculate the flow field for all x up to and including $T = 0.625$. At the next time interval, $T = 0.65$, calculations were performed without any signs of trouble up to and including $x = 0.85$ ($\equiv 153°$). At the next station, $x = 0.875$ ($\equiv 157°$), even though convergence was obtained, the asymptotic behavior of f'' was not satisfactory as $Y \to Y_\infty$, that is, $F''(Y_\infty)$ did not approach zero but began to grow. We observed the same behavior at the next station $x = 0.90$, before the solutions diverged at $x = 0.925$. At $T = 0.675$, the last "good" x-station prior to the unacceptable behavior of $F''(Y_\infty)$ was $x = 0.80$ ($\equiv 144°$), which decreased to $x = 0.775$ at $T = 0.70$ and to $x = 0.75$ at $T = 0.725$.

The next set of calculations were made by choosing t_* equal to $\frac{1}{4}$ and by using the same Δx, $\Delta\eta$, and Δt-spacing. Thus, in the first stage of the computation, flow reversal does not occur, and in the second stage, for $t > \frac{1}{4}$, the calculations were done by using the standard Box method with the zigzag differencing scheme. The solutions were obtained with the standard Box method when there were no regions of backflow, and were obtained by the zigzag differencing scheme when there were regions of backflow. For all practical purposes, the results obtained earlier by the standard Box scheme agreed extremely well with those obtained by the new procedure except now the solutions did not breakdown at those x-stations previously mentioned, and the calculations were performed up to $x = 1$ ($\equiv 180°$) for values of t up to 2.8. The calculations up to this t, although they were free of numerical difficulties and showed no signs of trouble, were terminated after this t due to the very rapid thickening of boundary-layer thickness with increasing t. For example at $x = 1$, the boundary-layer thickness Y_∞ was 10 at $t = 1.0$ and became 30 at $t = 2.5$. Since our ΔY spacing was set at 0.1, calculations required 101 y-points at $t = 1.0$ and 301 points at $t = 2.5$ making the computer storage excessive. Presently, studies are being conducted to handle the rapid thickening of the boundary layer at large times so as to extend the calculations to much larger values of t without recourse to excessive computer storage.

Figure 3 shows the local skin-friction coefficient c_f around the circular cylinder for different values of T ranging from 0.1 to 1.40. Here c_f is defined by

$$c_f = \frac{\tau_w}{\frac{1}{2}\rho u_\infty^2}. \tag{50}$$

The reference velocity u_∞ is taken equal to $1/\pi$ in order to compare the present predictions with the previous predictions. Note that as T increases, the zero-skin-friction point moves from $x = 180°$ to 106.5° at $T = 1.40$. According to the calculations made by Cebeci using the Box method for steady flows (see Cebeci and Smith [6]), the separation point on the circular cylinder is $x = 105°$, a value which agrees closely with Terrill's value. Thus, the present computed values of c_f approach

this steady-state value with increasing t. Comparison of c_f-values computed by Belcher *et al.* [2] (they present them for values of $T = 0.80$ and 1.0) and by Collins and Dennis [8, 9] (they present them for values of $T = 0.2$, 0.4, 0.6, 0.8, 1.0) and by Bar-Lev and Yang [1] shows that they are in excellent agreement with those computed by the present method for $0° \leqslant x \leqslant 180°$.

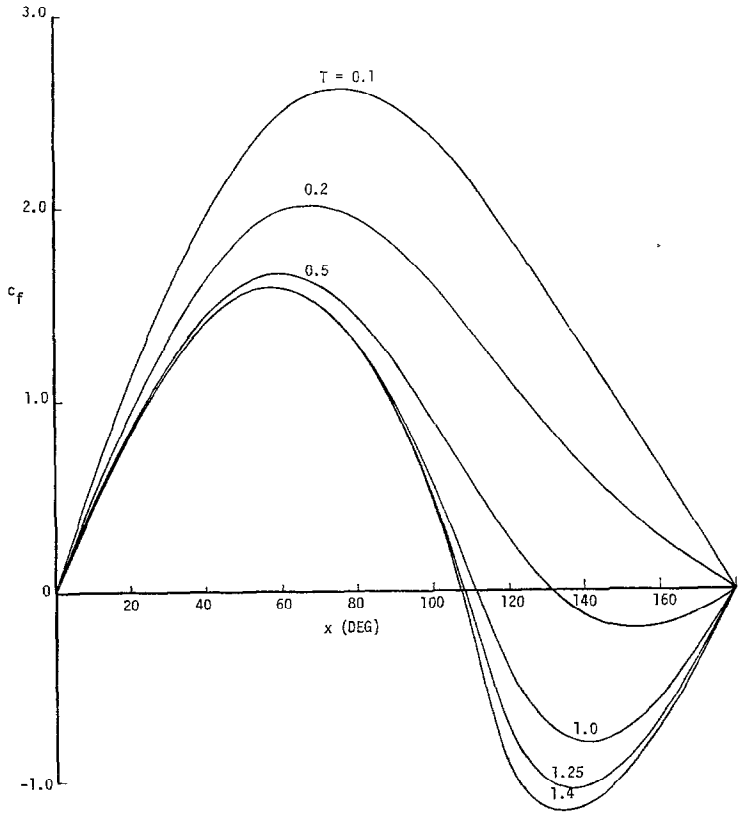

FIG. 3. Computed c_f values for the circular cylinder.

Figure 4 shows the dimensionless displacement thickness δ^*/L around the circular cylinder for different values of T ranging from 0.1 to 1.0. Here δ^* is defined by

$$\delta^* = \int_0^\infty (1 - u/u_e)\, dy. \tag{51}$$

Belcher *et al.* also computed the present δ^*/L values for $T \leqslant 0.70$ for all x and for $T = 1.0$ for x up to 130°. Comparison of our computed δ^*-values again agree quite well with their computed values.

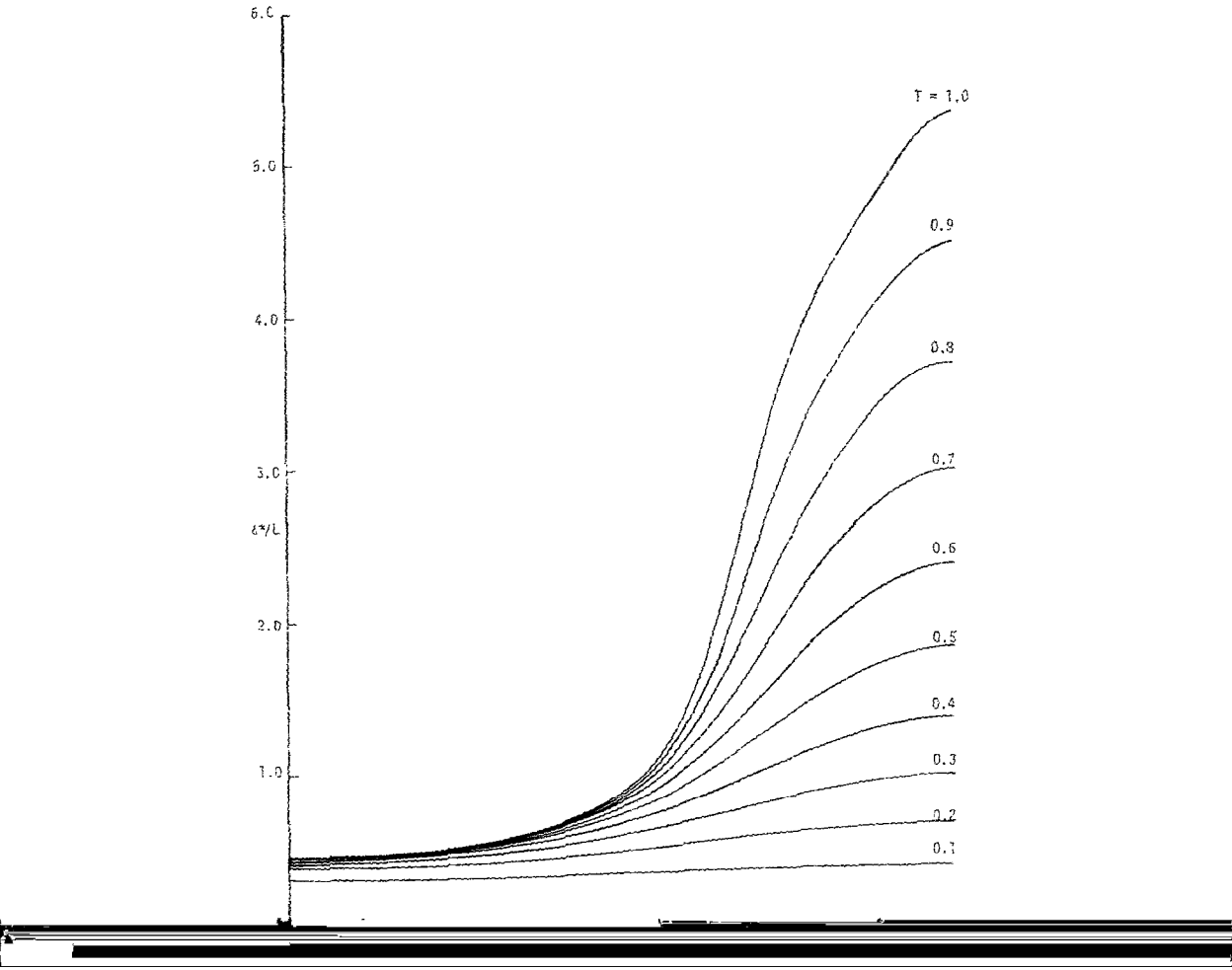

FIG. 4. Calculated displacement thickness values for the circular cylinder.

Figure 5 shows the variation of the wall-shear parameter F''_w at the forward ($x = 0$) and rear ($x = 1$) stagnation points as a function of time. Here F''_w is defined by

$$F''_w = \frac{L}{u_e}\left(\frac{\partial u}{\partial y}\right)_w. \tag{52}$$

As is seen, these results appear to agree reasonably well with the predictions of Proudman and Johnson [14] that the slope of the wall-shear parameter at $x = 0$ should tend to the same value as the slope at $x = 1$ as T becomes large. The results in Fig. 5a show that, at $x = 0$, F''_w reaches its steady state value of 1.23259 rapidly, whereas the results in Fig. 5b show that at $x = 1$ the approach of F''_w to its steady-state

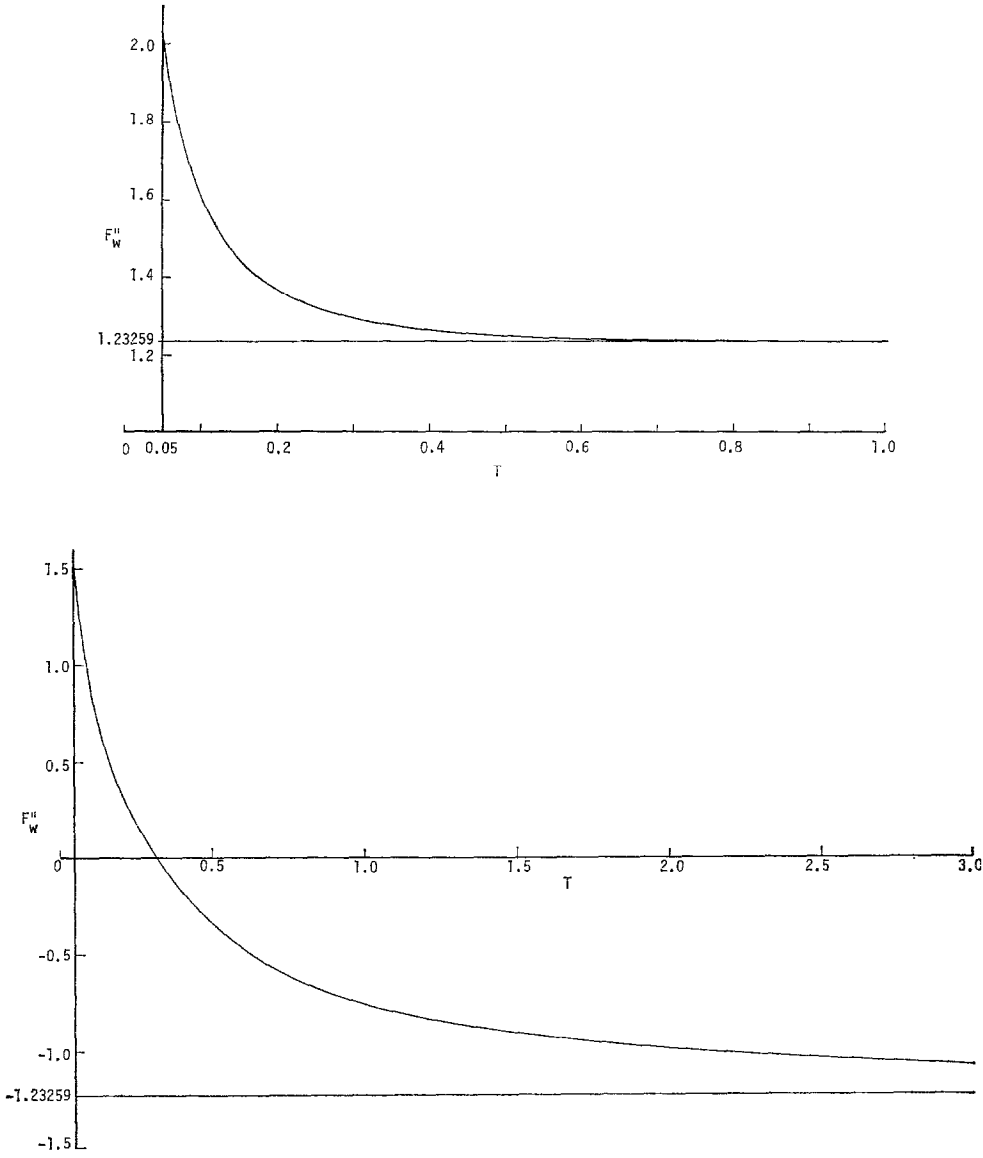

FIG. 5. Variation of wall shear parameter F''_w as a function of T. (a) Forward stagnation point ($x \equiv 0$); (b) rear stagnation point ($x \equiv 1$).

value is comparatively slow. It is noted that the wall shear first becomes zero at $T = 0.320$ close to that predicted by Goldstein and Rosenhead [10] ($T = 0.32$) and Bar-Lev and Yang [1] ($T = 0.322$), but significantly different from that by Telionis and Tsahalis [18] ($T = 0.35$).

Figure 6 shows the computed velocity profiles at various locations on the cylinder, including the rear stagnation point for various values of T. As is seen, the region of backflow is quite small at small values of x and T (as expected) and becomes quite large with increasing x and T.

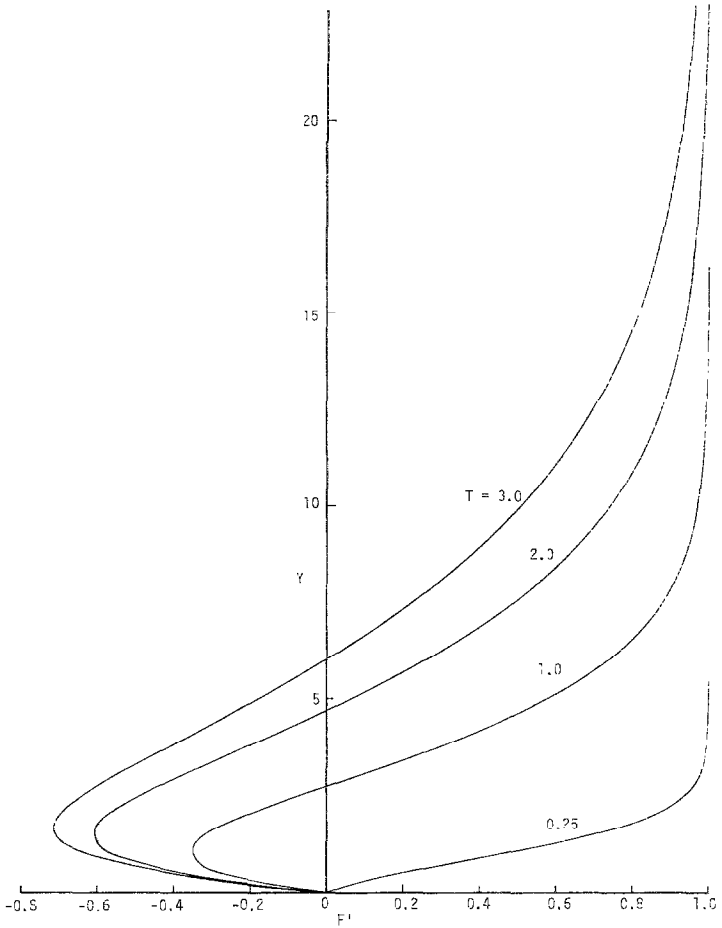

FIG. 6. Velocity profiles at the rear stagnation point.

Figure 7 shows the trajectory of the zero wall shear around the circular cylinder as a function of time for values of T up to 1.40. Also shown in Fig. 1 are the results of Telionis and Tsahalis [18]. We also show, in Fig. 1, the results obtained by the standard Box method for $0 < T < 0.75$. It is interesting to note that even the unmodified Box method can carry the calculations further downstream than those obtained by the numerical method used by Telionis and Tsahalis.

Bar-Lev and Yang [1] present a summary of zero wall shear as a function of angle

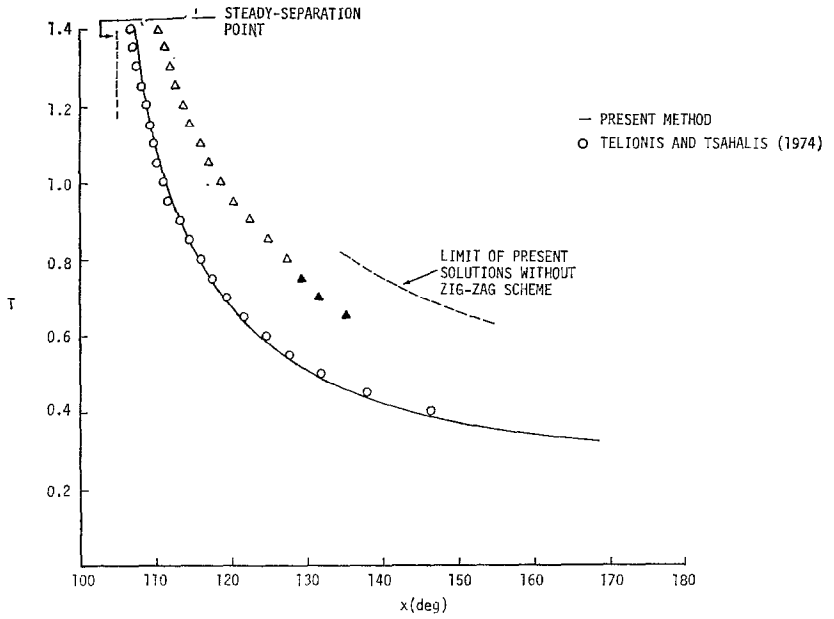

FIG. 7. Position of zero skin friction as a function of time. The symbols △ ▲ denote time and position where the solutions of Telionis and Tsahalis (1974) break down, the symbol ○ denotes the solutions of Telionis and Tsahalis (1974) for zero skin friction. No breakdown was observed in the present calculations.

TABLE I

Comparison of Zero Wall Shear around the Circular Cylinder

Investigator	180	166	146	138	124	110
Collins and Dennis [8]	0.322	0.331	0.39	0.43	0.589	0.90
Collins and Dennis [9]	0.322	0.33	0.39	0.42	0.59	1.10
Sears and Telionis [17]	0.35	0.36	0.40	0.45	0.60	1.11
Bar-Lev and Yang [1]	0.322	0.330	0.389	0.438	0.602	1.089
Present	0.320	0.330	0.390	0.436	0.596	1.10

and time as computed by Collins and Dennis [8, 9], Sears and Telionis [19], and by them. Table I shows a comparison of our calculated values with them. Overall the agreement is quite good except for the initiation of zero wall shear at the rear stagnation point.

Concluding Remarks

The new method of computation proposed here for boundary layers in which reversed crossflow can occur, namely, a combination of the Keller Box scheme with a zigzag procedure, has been applied to an equivalent problem—namely, the unsteady boundary layer over an impulsively started circular cylinder. At moderate times the results agree well with the previous studies reported by Proudman and Johnson [14], Belcher *et al.* [2], Collins and Dennis [8, 9], and Bar-Lev and Yang [1] and we are able to extend the calculations for the entire boundary layer to higher values of T than were possible previously. The difficulty about extending the computation even further is not now associated with flow reversal which the zigzag scheme seems to handle satisfactorily. The limitation is provided by the rapid increase of thickness of the boundary layer in the reversed flow region which makes the computations there increasingly uneconomical.

An important result of this paper is to reinforce the conclusions of the authors cited in the previous paragraph that this unsteady boundary layer is free of singularities for $T < 1.4$ and to suggest most strongly that it is smooth for all finite time even though its thickness is likely to increase exponentially for $\pi x > 1.82$. We contend, that, so far as unsteady boundary layers governed by the Eqs. (1)–(3) are concerned, there is no justification for the claim of Sears and Telionis [17] that they can develop a singularity at a finite value of T and that, on the contrary, solutions exist for all T. Consequently, the theory can be applied to such important problems of engineering design as dynamic stall provided a suitable method can be found to handle the exponential growth of the boundary-layer thickness and we shall investigate this in the near future.

References

1. M. Bar-Lev and H. T. Yang, Initial flow field over an impulsively started circular cylinder, *J. Fluid Mech.* **72** (1975), 625–647.
2. R. J. Belcher, O. R. Burggraf, J. C. Cooke, A. J. Robins, and K. Stewartson, Limitless boundary layers, *in* "Recent Research on Unsteady Boundary Layers," Proc. Int. Union Theoret. Appl. Mech. (E. A. Eichelbrenner, Ed.), pp. 1444–1466, 1971.
3. H. Blasius, Brenzschichten in Flussingkeiten mit kleiner Reibung, *Z. Math. Phys.* **56** (1908), 1–37. Also NACA, Tech. Memo. 1256.
4. R. J. Bodonyi and K. Stewartson, The unsteady laminar boundary layer on a rotating disk in a counter-rotating fluid, *J. Fluid Mech.* **79** (1977), 669–688.
5. L. W. Carr, K. W. McAlister, and W. J. McCroskey, Analysis of the development of dynamic stall based on oscillating airfoil experiments, NASA TN D-8382.
6. T. Cebeci and P. Bradshaw, "Momentum Transfer in Boundary Layers," McGraw-Hill–Hemisphere, Washington, D. C., 1977.
7. T. Cebeci and A. M. O. Smith, "Analysis of Turbulent Boundary Layers," Academic Press, New York, 1974.
8. W. M. Collins and S. C. R. Dennis, The initial flow past an impulsively started circular cylinder, *Quart. J. Mech. Appl. Math.* **26** (1973), 53–75.

9. W. M. COLLINS AND S. C. R. DENNIS, Flow past an impulsively started circular cylinder, *J. Fluid Mech.* **60** (1973), 105–127.
10. S. GOLDSTEIN AND L. ROSENHEAD, Boundary-layer growth, *Proc. Cambridge Philos. Soc.* **32** (1936), 392–401.
11. H. B. KELLER, Accurate difference methods for two-point boundary-value problems. *SIAM J. Numer. Anal.* **11** (1974), 305–320.
12. E. KRAUSE, E. H. HIRSCHEL, AND TH. BOTHMANN, Die numerische integration der bewegungsgleichungen dreidimensionaler laminarer kompressibler grenzschichten, Bond 3, Fachtagung Aerodynamik, Berlin, 1968; D6LR–Fachlinchreike.
13. J. H. PHILLIPS AND R. C. ACKERBERG, A numerical method for integrating the unsteady boundary-layer equations when there are regions of backflow, *J. Fluid Mech.* **58** (1973), 561–579.
14. I. PROUDMAN AND K. JOHNSON, Boundary-layer growth near a rear stagnation point, *J. Fluid Mech.* **14** (1962), 161–168.
15. N. RILEY, Unsteady laminar boundary layers, *SIAM Rev.* **17** (1975), 274.
16. W. R. SEARS AND D. P. TELIONIS, Unsteady boundary-layer separation, *in* "Recent Research on Unsteady Boundary Layers," Proc. Intl. Union Theoret. Appl. Mech., (E. A. Eichelbrenner, Ed.), pp. 404–447.
17. W. R. SEARS AND D. P. TELIONIS, Boundary-layer separation in unsteady flow, *SIAM J. Appl. Math.* **28** (1975), 215.
18. D. P. TELIONIS AND D. T. TSAHALIS, Unsteady laminar separation over cylinder started impulsively from rest, *Acta Astronautica* **1** (1974), 1487.
19. R. M. TERRILL, Laminar boundary-layer flow near separation with an without suction, *Philos. Trans. Roy. Soc. London Ser. A.* **253** (1960), 55–100.
20. D. C. THOMAN AND A. A. SZEWCZYK, Time-dependent viscous flow over a circular cylinder. High-Speed Computing in Fluid Dynamics, *Phys. Fluids Supp.* II (1969), II-76/II-86; also Univ. of Notre Dame, Notre Dame, Ind. Tech. Rept. 66-14, 1966.
21. J. C. WILLIAMS, III, *Annual Rev. Fluid Mech.* **9** (1977).